J. Fluid Mech. (1972), *vol.* 55, *part* 3, *pp.* 401–417
Printed in Great Britain

Self-induced oscillations in an open water-channel with slotted walls

By P. L. BETTS

Department of Mechanical Engineering, The University of Manchester Institute of Science and Technology

(Received 8 August 1971 and in revised form 23 May 1972)

Previous experiments on a small-scale rectangular water-channel with slotted walls revealed that under certain circumstances the flow could become unsteady. Although these oscillations were suppressed at the time, the mechanism of the instability was not fully understood. Theoretical work, on a similar form of instability in a circular slotted-wall wind tunnel, has been extended to describe the oscillations in the water channel. Further experiments have been performed, and in some of these the length of the outer chamber surrounding the working section was altered. Good agreement between the theoretical and experimental results was obtained. Consideration has also been given to the occurrence of the self-induced oscillations in flumes of different scale and form.

1. Introduction

Experimental work by Betts & Binnie (1966) and Binnie & Cloughley (1970) has demonstrated that larger models can be satisfactorily accommodated in an open water-channel if the walls and bottom of the channel contains longitudinal slots which connect the working section to a large open reservoir surrounding the channel and containing effectively stationary water. In the earlier work, a form of self-induced oscillation was reported. This consisted of a longitudinal standing wave oscillation (first 'sloshing' mode) in the outer chamber, with the surface variations in phase across the outer chamber and the slotted working section; the amplitude of the standing wave was slightly larger in the working section than at the same longitudinal position in the outer chamber. Although the instability was eliminated at the time, it appeared worthwhile to investigate this further to gain a better understanding of the mechanism involved and to determine the likelihood of its occurrence in a larger scale channel.

The experiments described in this paper were performed in the same small channel as before. This had a $14\frac{1}{8}$ in. wide slotted-wall working section, just under 6 ft long, followed by a solid wall section about 2 ft long. In addition, a false end wall was constructed which, when fitted at the downstream end, reduced the length of the outer chamber from 8 ft to just over 6 ft. Comparisons were made with an extension of the theory for similar oscillations in a slotted-wall wind tunnel; the results seem to be sufficiently in agreement for forecasts to be made of the regions in which such oscillations are liable to occur in channels of different design and scale.

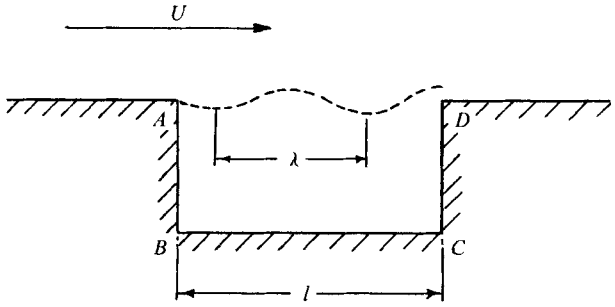

FIGURE 1. Self-induced oscillations with air flow across a rectangular cavity.

2. Theoretical considerations of the mechanism of instability

2.1. *General considerations*

The way in which a basic hydrodynamic instability can develop into a finite amplitude oscillation, with little harmonic content, when a feed-back mechanism is present has been well described in a general report by Naudascher (1967). The most relevant case of this kind of flow-induced excitation is illustrated in figure 1, where a uniform air flow passes over a rectangular cavity $ABCD$ in the side wall (cf. Rossiter 1966; East 1966). At the upstream end A, perturbations will develop over a wide range of frequencies, owing to the hydrodynamic instability of the shear layer between the main flow and the almost stationary fluid in the cavity. These perturbations will amplify and be convected downstream, at the rates appropriate to their wavelengths, until they reach the downstream end D, where they experience a constraint; a force is therefore exerted on the fluid and induces additional velocity and pressure disturbances. These pressure disturbances, which are transmitted at sonic speed throughout the flow field, have the greatest effect at the sensitive upstream end A and produce new perturbations there. Some of these new perturbations will be in phase with the original perturbation pattern; the subsequent perturbations at these frequencies will therefore be more intense and lead to stronger disturbances at D. The perturbations will thus continue to grow, becoming more and more periodic and intense, until a state of equilibrium is reached between amplification and dissipation and an almost steady-state oscillation of the flow is obtained. The large amplitude oscillations thus occur in a narrow frequency band and not randomly as in turbulence.

For the cavity system under consideration, Rossiter found that, provided the shear layer did not reattach to the rear wall BC, a phase shift of about $\frac{3}{4}$ cycles along the mouth of the cavity provided optimum feed-back when the mainstream velocity was at sufficiently low Mach number for the sonic speed of the pressure disturbances to be much larger than the convection velocity of the shear-layer perturbations. Moreover, the feed-back mechanism may involve a resonance of some form, for instance, an organ-pipe resonance of the open-ended cavity (as in East's experiments) or a mechanical resonance of the backing plate BC. The feed-back will then be dominated by this, and the self-induced oscillations will appear only at frequencies close to the natural frequency of resonance or its harmonics, if they exist. Thus,

$$l/\lambda \simeq N - \tfrac{1}{4} \tag{1}$$

and
$$f = c_r/\lambda \simeq f_n, \tag{2}$$

where l is the length of the cavity AD, λ the wavelength of the shear-layer disturbance, f the frequency and c_r the mean convection or phase velocity. N is a positive integer and f_n a natural frequency of the resonator. Thus, since the ratio of c_r to the mainstream velocity U depends on the wavelength of the perturbation, the large self-induced oscillations will occur at certain specific velocities which could be calculated if the dependence of c_r/U or λ were known.

King, Boyle & Ogle (1958) observed self-induced oscillations caused by resonant feed-back in a circular slotted-wall subsonic wind tunnel and successfully calculated the convection velocity from the theory of hydrodynamic stability. They also confirmed that the oscillating pressure was in phase throughout the outer chamber and that the phase change of the convected perturbation along the length of the working section was $\frac{3}{4}$ cycles†. The resonance could have been mechanical, but it is more likely that the passages into the working section, provided by the slots, allowed the outer chamber to act as a Helmholtz resonator.

2.2. *The theory for a circular slotted-wall wind tunnel*

King *et al.* assumed that the effects of the slats and gaps in the slotted wall could be averaged round the circumference, a common assumption in the theory of slotted-wall wind tunnels originated by Baldwin, Turner & Knechtel (1954). Furthermore, they were able to neglect the effects of the thickness of the shear layer between the mainstream and the outer chamber, since its growth was restricted by the slats and its dimensions were always small compared with the wavelength of the disturbance. Thus, the problem became the familiar one of the instability of a circular jet of incompressible fluid, of radius R_1, moving with velocity U through a body of the same fluid at rest and bounded by a solid boundary at radius R_2 ($R_2 > R_1$) (Rayleigh 1879). Only axisymmetric disturbances were considered, since only these could operate the feed-back mechanism. The average effect of the slats was to impose a pressure difference across the disturbed boundary of the jet, but King *et al.* found that this had a negligible effect on the convection velocity in their slotted-wall tunnel; this was to be expected as the 20 % open-area ratio of the tunnel had been chosen to give the same model blockage interference as an ideal open jet (Vandrey & Wieghardt 1955).

Following King *et al.* consider the common surface of the mainstream and the surrounding fluid to be at radius

$$r = R_1 + \eta,$$

where η is small and a function of downstream distance z and time t. The velocity potential takes the form

$$\Phi = \begin{cases} -Uz + \phi \text{ inside the jet,} \\ \phi' \text{ outside the jet,} \end{cases} \tag{3}$$

† Care must be taken to distinguish between the gross disturbance, which was in phase throughout the outer chamber (and the working section), and the smaller progressive wave, in the shear layers between the slats, which activated it.

where ϕ and ϕ' are the small disturbance potentials associated with η which must individually satisfy Laplace's equation. The disturbance considered is a progressive wave moving downstream of the form

$$\eta = \eta_0 \exp[i(\omega t - kz)], \tag{4}$$

and so the required solutions of Laplace's equation are

$$\left.\begin{aligned} \phi &= [CI_0(kr) + C'K_0(kr)] \exp[i(\omega t - kz)], \\ \phi' &= [DI_0(kr) + D'K_0(kr)] \exp[i(\omega t - kz)]. \end{aligned}\right\} \tag{5}$$

These are complex expressions from which the imaginary parts will be rejected later, and I_0 and K_0 are modified Bessel functions of order zero defined by Watson (1944).

There are five boundary conditions to be satisfied; zero radial velocity at $r = 0$ (i.e. $C' = 0$) and at $r = R_2$, and two kinematic conditions and a continuity of pressure condition on the common surface $r = R_1$ (since $\eta \ll R_1$). After elimination of the remaining constants C, D' and D, the resulting equation to be satisfied is

$$(X-1)^2 + \alpha X^2 = 0, \tag{6}$$

where

$$X = \omega/kU$$

and

$$\alpha = \frac{I_1(kR_1)\,K_0(kR_1)}{I_0(kR_1)\,K_1(kR_1)} \left[\frac{1 + K_1(kR_2)\,I_0(kR_1)/I_1(kR_2)\,K_0(kR_1)}{1 - K_1(kR_2)\,I_1(kR_1)/I_1(kR_2)\,K_1(kR_1)}\right].$$

The quantity α is a function of kR_1 and R_2/R_1 only, and as R_2/R_1 tends to infinity the term within the square brackets tends to unity (i.e. $D \to 0$).

The solution of (6) is complex ($X = X_1 + iX_2$), except when $k = 0$. Thus for any particular value of R_2/R_1 and a chosen value of k_1 ($= 2\pi/\lambda$), there is an infinite number of possible values of $k = k_1 + ik_2$, to each of which corresponds a value of $\omega = \omega_1 + i\omega_2$, and η contains a real exponential factor $\exp(-\omega_2 t + k_2 x)$. The disturbance therefore grows with time if $\omega_2 < 0$ and with distance downstream if $k_2 > 0$, and the ratio of convection velocity to mainstream velocity is

$$f\lambda/U = \omega_1/k_1 U.$$

In the past (Lin 1955) it was assumed that the convection velocity was unaffected by the form of the growth (i.e. $k_2 = 0$, purely temporal growth; or $\omega_2 = 0$, purely spatial growth). However, it is now known that this is generally not so, and for axisymmetric disturbances, Umiastowski (1969) has shown that the convection velocity for spatial growth is greater than that for temporal growth, except when $k_1 R_1$ is zero.† Consideration of the initial stages of the growth of the self-induced oscillation discussed in § 2.1 suggests that, if the feed-back mechanism is efficient, the value of k_2 will be small in comparison with $-\omega_2$ (or more particularly $k_2/k_1 \ll -\omega_2/\omega_1$). Thus in the present case we would expect a convection velocity only marginally above that corresponding to temporal growth, and consequently

$$\frac{f\lambda}{U} \simeq \frac{\omega_1}{kU} = X_1 = \frac{1}{1+\alpha}. \tag{7}$$

† Confirmation of this is available from the recent independent work of Crow & Champagne (1971).

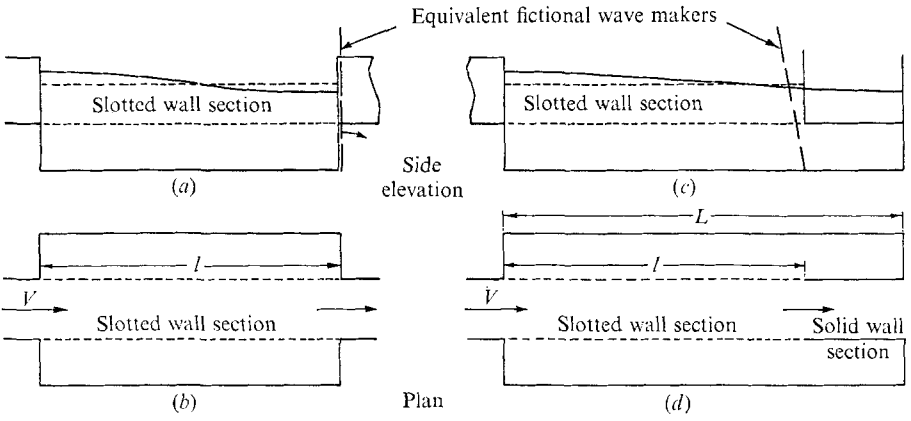

FIGURE 2. Configurations for self-induced oscillations in a slotted-wall flume; (*a*), (*b*) short outer chamber; (*c*), (*d*) long outer chamber. The broken lines in (*a*) and (*c*) indicate the region occupied by the longitudinal slats; the mean of the water surface level sketched in these figures lies slightly above the top slat.

King *et al.* considered only the case of temporal growth but retained a term in their equations to account for the possible pressure difference across the slats. They showed that, for a growing disturbance, the effect of this term would be to reduce the convection velocity, but that, for their experimental conditions, this effect was negligible. The above analysis has been based on linearized inviscid theory. Lin (1955, §8.3) has shown that inviscid theory is the proper limiting condition as viscous effects tend to zero, provided that the disturbance is amplifying; moreover, there is experimental and theoretical evidence (Rosenhead 1931; Sato 1956, 1959) that the phase velocity (but not the growth rate) will be correctly predicted by linearized theory up to quite large amplitudes, even in the absence of the tuning effect described in §2.1. However, the use of the theory described in this section must finally rest on the experimental results of King *et al.*

2.3. *Extension of the theory to the slotted-wall rectangular flume*

In the slotted-wall tunnel, described above, the pressure was in phase throughout the outer chamber. However, in the slotted-wall flume, the gross oscillation observed by Betts & Binnie (1966) was a standing wave along the outer chamber. The length of the standing wave was approximately twice the length of the outer chamber, and the surface level had a single central node. Thus the pressure in the upstream half of the chamber was π out of phase with that in the downstream half, and for a flume with the same configuration as the tunnel (figures 2(*a*) and (*b*)), one would now expect

$$l/\lambda \simeq N - \tfrac{3}{4}, \tag{8}$$

where λ is again the wavelength of the convected shear-layer disturbance. The finite amplitude of the standing waves would not alter the natural frequency significantly, for the amplitudes and ratios of length to depth observed, but the work of Fultz (1962) suggests that a soft or damped resonance would be expected (i.e. amplitude not drastically reduced when slightly off resonance). For the situation shown in figure 2(*a*), a fictional wave maker, oscillating at the

natural frequency and situated at the downstream end, would be passing through its centre position moving outwards at the moment when the elevation of the standing wave was a maximum at the upstream end. The phase of this imaginary wave maker must be fixed relative to the phase of the shear-layer disturbance at the downstream end of the slotted section. However, for the situation illustrated in figure 2 (*d*), where the outer chamber extends significantly beyond the end of the slotted section, the equivalent fictional wave maker in figure 2(*c*) is no longer near the end wall, although it is still situated in the downstream half of the outer chamber. It would therefore be at its maximum inward inclination when the surface elevation of the standing wave was a maximum at the upstream end and consequently retarded by $\frac{1}{2}\pi$ relative to a wave maker situated at the downstream end wall (cf. figure 2 (*a*))†. One is therefore led to expect that for the experimental conditions of figure 2 (*d*) the wavelength of the convected shear-layer disturbance is given by

$$l/\lambda \simeq N - \tfrac{1}{2}. \tag{9}$$

An attempt must now be made to calculate the phase velocities of the shear-layer disturbances in the rectangular flume. Since there is no analytic theory available even for a rectangular tunnel, a heuristic approach must be adopted. An initial consideration of the experimental evidence from the slotted flume shows that, for any reasonable estimate of the phase velocity, the length of the shear-layer disturbance must be more than the width of the working section. Consequently, as in the work of King *et al.* the size and shape of the cross-section of the main flow will be significantly more important than the thickness of the shear layer or the spacing of the slats (provided that the open-area ratio is sufficiently large). However, for values of kR_1 which are not too large (order unity or less), the streamwise perturbation velocity $-\partial\phi/\partial z$ in the circular slotted tunnel can be shown to be almost uniform across the working section. Thus, with the value of the constant C inserted in equation (5),

$$-\frac{\partial\phi}{\partial z} = -(kU-\omega)\frac{I_0(kr)}{I_1(kR_1)}\eta_0 \exp[i(\omega t - kz)]$$

$$= \frac{-2(kU-\omega)\,I_0(kr)\,\eta_0 \exp[i(\omega t - kz)]}{kR_1 I_0(kR_1)\,[1 - I_2(kR_1)/I_0(kR_1)]}.$$

Moreover, for kR_1 not too large,

$$I_0(kr)/I_0(kR_1) \simeq 1$$

and

$$I_2(kR_1)/I_0(kR_1) \simeq 0,$$

† The situation considered here, with the frequency and wavelength of the standing wave remaining in effect fixed while the wave maker is moved, is directly comparable with that described by Taylor (1953), where the position of the wave makers was fixed but the frequency, and consequently the wavelength, of the standing wave was varied. The phase of a wave maker then changed by fully π radians relative to the surface oscillation as the frequency changed from below to above the resonant frequency. It can readily be confirmed experimentally that, for the large ratios of wavelength to depth being considered here, the relative phase of a wave maker advances smoothly through $\frac{1}{2}\pi$ radians at resonance as the frequency is increased.

since $kr \leqslant kR_1$. Consequently,

$$-\frac{\partial\phi}{\partial z} \simeq \frac{-2(U-\omega/k)\eta_0}{R_1}\exp[i(\omega t-kz)], \tag{10}$$

which is independent of radial position across the tunnel. Hence under these conditions, where the perturbation flow is effectively one-dimensional, one would expect the instability characteristics not to depend critically on the shape of the tunnel but to depend only on a single linear dimension which describes its size.

For a rectangular flume, the gravitational effect complicates the situation. However, a one-dimensional analysis can still be made of the fluctuations in the mainstream. Consider a rectangular channel of mean depth d, mean width b and mean velocity of water $\overline{V}$. Following the method of § 2.2, we define a velocity potential such that

$$\Phi = \phi_0\exp[i(\omega t-kz)] - \overline{V}z,$$

where ϕ_0 is effectively independent of position across the stream but, as before, may be complex. Consequently, the local streamwise velocity V at any cross-section is given by

$$V = -\partial\Phi/\partial z = ik\phi_0\exp[i(\omega t-kz)]+\overline{V}. \tag{11}$$

Continuity considerations across adjacent cross-sections lead to

$$\left(V+\frac{\partial V}{\partial z}\delta z\right)\left(A+\frac{\partial A}{\partial z}\delta z\right)-VA+\frac{\partial A}{\partial t}\delta z = 0,$$

where A is the local cross-sectional area, or

$$A\frac{\partial V}{\partial z}+V\frac{\partial A}{\partial z}+\frac{\partial A}{\partial t} = 0, \tag{12}$$

when second-order terms are neglected. A must take the form

$$A = A_0\exp[i(\omega t-kz)]+\bar{A},$$

where $\bar{A}$ is the mean cross-sectional area bd. Hence, combining (11) and (12) and neglecting second-order terms leads to the requirement

$$\bar{A}k\phi_0 - iA_0(\overline{V}-\omega/k) = 0.$$

Let the variations in cross-sectional area be caused by displacements η of the common surfaces between the mainstream and the surrounding fluid given by

$$\eta = \eta_0\exp[\mathrm{i}(\omega t-kz)],$$

and vertical displacements δh of the free surface such that

$$\delta h = (\delta h)_0\exp[i(\omega t-kz)],$$

with δh measured positive upwards and η positive outwards. Then,

$$A_0 = (2d+b)\eta_0+b(\delta h)_0,$$

and consequently,

$$\bar{A}k\phi_0 - i[(2d+b)\eta_0+b(\delta h)_0](\overline{V}-\omega/k) = 0. \tag{13}$$

Now, Bernoulli's equation for unsteady flow gives

$$\partial\Phi/\partial t - g\,\delta h - \tfrac{1}{2}V^2 = \text{constant}$$

for the conditions considered. Thus, equating the fluctuating parts of the left-hand side to zero and neglecting second-order terms leads to

$$(\delta h)_0 = -(ik\phi_0/g)\,(\bar{V} - \omega/k). \tag{14}$$

When this is combined with (13), we obtain

$$\phi_0 = \frac{i(2d+b)\,(\bar{V}-\omega/k)\,\eta_0}{k[\bar{A} - b(\bar{V}-\omega/k)^2/g]}$$

and the following for the fluctuating component of the mainstream velocity:

$$ik\phi_0 \exp[i(\omega t - kz)] = \frac{-(2d+b)\,(\bar{V}-\omega/k)}{bd\,[1-(\bar{V}-\omega/k)^2/gd]}\,\eta_0 \exp[i(\omega t - kz)]. \tag{15}$$

A comparison of (10) and (15) suggests that, within the range of wavenumbers where the perturbations are effectively one-dimensional, the convection velocities in the slotted flume may be calculated from the theory for a slotted circular tunnel of 'equivalent radius'

$$R_1 = \frac{2bd}{2d+b}\left[1 - \frac{\bar{V}^2}{gd}\left(1 - \frac{\omega}{k\bar{V}}\right)^2\right]. \tag{16}$$

In temporal growth theory, the right-hand side of (16) contains an imaginary term due to the presence of the complex frequency $\omega = \omega_1 + i\omega_2$; this would lead to the impossible situation of a complex 'equivalent radius'. However, within the range of wavenumbers of interest, the second term within the square brackets is always negligibly small compared with unity. Moreover, calculations based on the theoretical values of ω_1 and ω_2 for the ideal circular jet show that when the imaginary part starts to be significant it is of the same order as the real part of the second term, which is of order $(\bar{V}^2/gd)\,(1-\omega_1/k\bar{V})^2$. Thus,

$$R_1 = 2bd/(2d+b) \tag{17}$$

provided that $(\bar{V} - \omega_1/k)^2/gd \ll 1$.

Elimination of ϕ_0 from (14) shows that

$$(\delta h_0) = \frac{(2d+b)}{b}\,\frac{(\bar{V}-\omega/k)^2/gd}{[1-(\bar{V}-\omega/k)^2/gd]}\,\eta_0.$$

Thus, when (17) is valid, $(\delta h)_0 \ll \eta_0$ and changes in the surface level caused directly by the progressive wave in the shear layer are negligible. The flume is therefore equivalent to half of a rectangular slotted tunnel of width b and depth $2d$. Equation (17) can easily be recognized as the definition of 'hydraulic mean radius', a concept which has been found useful in correlating friction factors in pipes of non-circular cross-section.

The fluctuating velocity $-\partial\phi'/\partial z$ in the outer chamber decreases rapidly with distance outwards and cannot be considered one-dimensional. Fortunately the size of the outer chamber in the experiments was always sufficiently large for the effects of the outer walls to be small, so the choice of the correct value for the

'equivalent radius' R_2 of the outer chamber is not critical. It is therefore reasonable to assume, by comparison with (17), that

$$R_2 = 2BD/(2D+B), \tag{18}$$

where B and D are the width and depth of the outer chamber respectively.

Extreme accuracy cannot be expected from the calculations of convection velocities in the slotted flume based on this heuristic approach of an equivalent circular tunnel. However, if the results are found to be within say 10 % of the correct value, the theory will have served its purpose and a considerable improvement will have been gained over the only alternative, namely guessing the convection velocity.

3. Description of apparatus and instruments

The apparatus was the same as that described by Betts & Binnie (1966). Water was supplied to the upstream end of a long open stilling section, from which it passed through a contraction to the slotted rectangular working section, along a short solid walled exit section and over a weir to the sump. The $14\frac{1}{8}$ in. wide working section was surrounded by a rectangular outer chamber 36 in. wide, the bottom of which was 10·77 in. below the bottom of the working section. The slotted section was 5ft $10\frac{1}{8}$ in. long and started 1·70 in. after the upstream end of the outer chamber. The basic outer chamber was 8 ft long; however, a solid false end plate was fitted at the downstream end for some experiments and the length of the outer chamber was then 6 ft $1\frac{3}{4}$ in. For all the experiments on self-induced oscillations the gaps between the slats were 0·4 in. (i.e. the nominal open-area ratio was $\frac{1}{6}$).

The amplitude and mean level of the free surface were measured with a point gauge on the centre-line of the apparatus and 2·50 in. downstream from the start of the slotted section. The stream velocities were measured with a miniflowmeter, but instead of counting pulses on a Dekatron chain, the speed of rotation of the miniflowmeter was read directly on a milliammeter by means of an electronic circuit similar to that described by Edington & Molyneux (1960). For convenience of mounting, the miniflowmeter was positioned 4·90 in. downstream from the pointer with the head at half the depth of the water in the working section. In the previous experiments the velocities had been measured with a total-head Pitot tube, positioned slightly closer to the start of the slotted section. The miniflowmeter was therefore occasionally moved upstream to the position previously occupied by the Pitot tube, and although the measured velocities were then in general marginally higher, the differences were always well within experimental error. Before use, the miniflowmeter and its associated circuitry were calibrated in the small circular calibration tank at H.R.S. Wallingford. Thereafter, confirmation was obtained by means of a hand-held transparent total-head tube and by observation of the onset of surface-tension ripples. All experimental readings were taken within three weeks of the initial calibration.

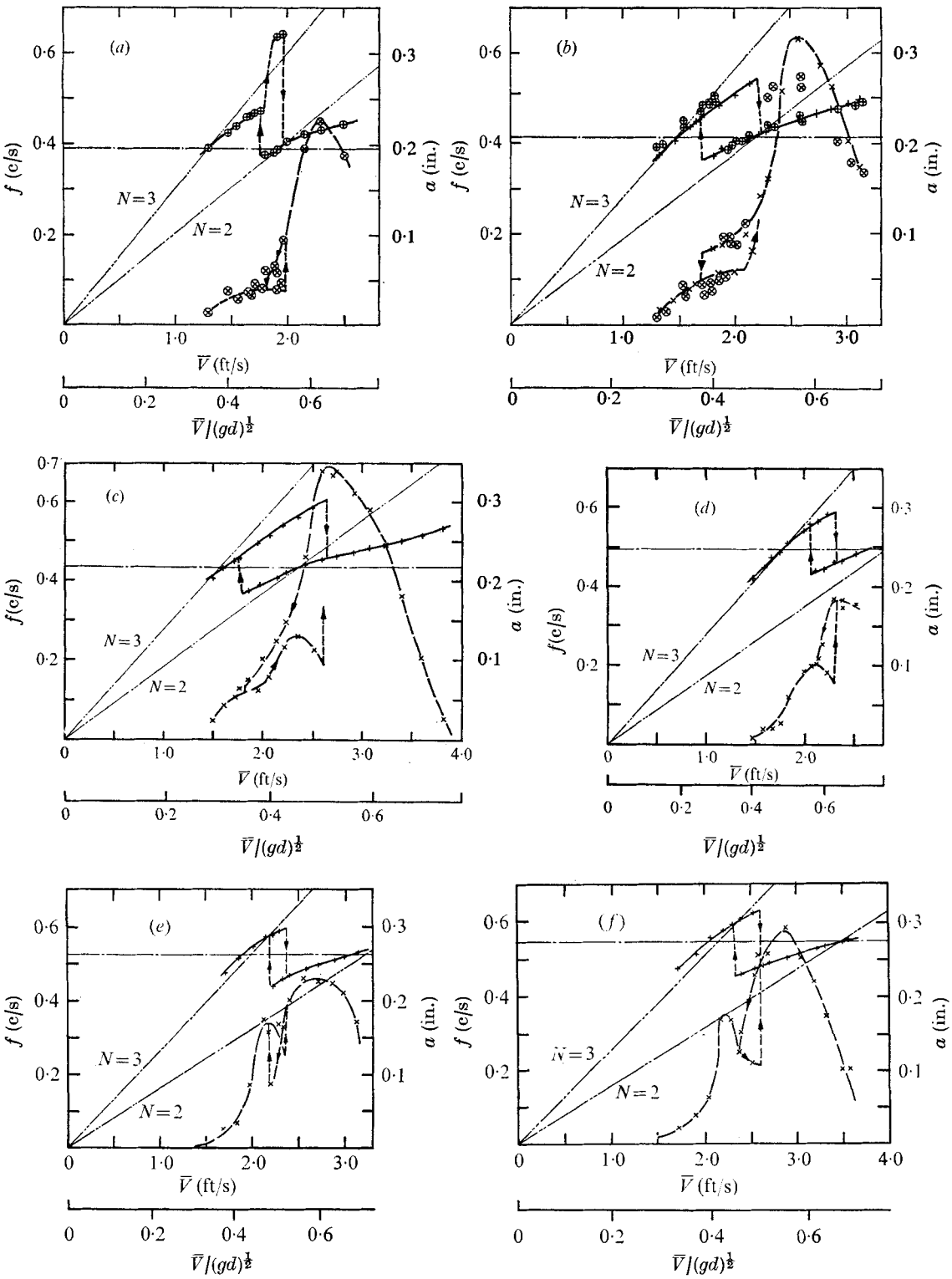

FIGURE 3. Variation of frequency f and amplitude a of oscillations with stream velocity $\bar{V}$. Long outer chamber: (*a*) $d = 5{\cdot}03$ in., (*b*) $d = 7{\cdot}63$ in., (*c*) $d = 10{\cdot}01$ in. Short outer chamber: (*d*) $d = 5{\cdot}02$ in., (*e*) $d = 7{\cdot}61$ in., (*f*) $d = 10{\cdot}01$ in. Frequency: ———, +, velocities measured with miniflowmeter; ⊕, velocities measured with Pitot tube. Amplitude: — —, ×, velocities measured with miniflowmeter; ⊗, velocities measured with Pitot tube. —·—, theoretical natural frequency, $f_0 = [(g/4\pi L)\tanh(\pi D/L)]^{\frac{1}{2}}$ of longitudinal standing wave; —··—, equation (20) for mode numbers N in (8) or (9).

4. Experimental results and comparisons with theory

Readings of the frequency and amplitude of the standing waves were taken over a range of stream velocities at two working section depths, $d = 7{\cdot}63$ and $10{\cdot}01$ in., with the long outer chamber (total length $L = 8$ ft) and at three depths, $d = 5{\cdot}02$, $7{\cdot}61$ and $10{\cdot}01$ in., with the short outer chamber ($L = 6$ ft $1\frac{3}{4}$ in.). The results are displayed on figures 3(*b*)–3(*f*), where the amplitude a is defined as half the height between a crest and a trough and the velocity is taken as the mean of the maximum and minimum indications on the milliammeter. The horizontal lines on the figures indicate the appropriate natural frequencies of small standing waves along the outer chamber. For completeness, the results from the previous experiments with a Pitot tube are displayed on figures 3(*a*) and 3(*b*). For most of these earlier experiments half ellipses were inserted at the downstream end of the slotted section, which shortened it by $\frac{3}{4}$ in. The agreement between the two series of experiments, as shown by figure 3(*b*), is very good, and the break in the frequency curve and the hysteresis effect were again observed; the slight discrepancy in the maximum amplitude is probably due to the earlier point gauge being rather blunt. The curves shown on figure 3(*b*) are those appropriate to the present experiments.

The essential results from figure 3 are summarized in table 1. It is noticeable that the maximum wave amplitudes with the long outer chamber occurred at velocities and frequencies higher than those associated with the natural frequency, whereas the reverse was true with the short outer chamber. Moreover, the smaller maximum amplitudes with the short chamber also occurred at velocities and frequencies higher than those associated with the first crossing of the natural frequency; the equivalent maxima with the long chamber were too indeterminate to measure. Discrepancies of this order are not unusual, as can be seen from the papers of East (1966) and Naudascher (1967).

The experimental results can most conveniently be compared with the theory at the natural frequencies of longitudinal oscillation, since these are the only frequencies known in advance by a designer.† The following approach was there-

† The natural frequency has been taken as the fundamental frequency of free small standing waves in a simple tank, with the same conditions of length and water depth as the outer chamber (f_0 on table 1). Apart from the question of the finite amplitude of the standing waves, which has been considered in § 2.3, there are at least two possible reasons why the maximum amplitude oscillations might not occur exactly at this natural frequency. First, the energy available for forcing the oscillation is likely to increase with the velocity of the water in the slotted channel; this effect would tend to increase the frequency of maximum amplitude oscillations above the natural frequency f_0 by an indeterminable amount which depends on the softness of the resonance. Second, the presence of the mainstream bounded by the slotted walls along the length of the tank is likely to alter the true natural frequency in an incalculable way. Intuitively one might expect this effect to be less with the long chamber, where the mainstream was bounded by a solid wall in the downstream quarter of the outer chamber. Similar effects would have been apparent in the other cases of resonant feed-back which have been considered, and they would have been a major cause of the discrepancies which have been noted. In the present experiments, oscillations, and even maximum amplitude oscillations, were observed with frequencies on both sides of the idealized natural frequency f_0. It is therefore reasonable to use f_0, the only frequency known in advance of the experiments, as a basis for comparison.

	Long outer chamber				Short outer chamber		
Designation on figure 3	(*a*)†	(*b*)†	(*b*)	(*c*)	(*d*)	(*e*)	(*f*)
Mean depth d (in.) over bottom slats	5·03	7·63	7·63	10·01	5·02	7·61	10·01
Mean depth D (in.) over bottom of outer chamber	15·83	18·43	18·40	20·78	15·79	18·38	20·78
Theoretical natural frequency $f_0 = [(g/4\pi L) \tanh (\pi D/L)]^{\frac{1}{2}}$ (c/s) of longitudinal standing wave	0·390	0·416	0·415	0·435	0·494	0·523	0·544
Higher velocity $\bar{V}_1$ (ft/s) at which frequency $= f_0$	1·90	2·18	2·18	2·37	2·64‡	3·04	3·44
Lower velocity $\bar{V}_2$ (ft/s) at which frequency $= f_0$	1·29	1·46	1·52	1·62	1·77	1·88	2·03
Frequency of maximum amplitude oscillations (c/s)	0·431	0·444	0·449	0·457	0·465	0·495	0·502
Velocity for maximum amplitude oscillations (ft/s)	2·29	2·49	2·55	2·66	2·36	2·69	2·86
Frequency of smaller maximum amplitude oscillations (c/s)	—	—	—	—	0·563	0·578	0·581
Velocity for smaller maximum amplitude oscillations (ft/s)	—	—	—	—	2·12	2·20	2·24

† Velocities measured with a Pitot tube.

‡ This value occurs slightly above the range of the experimental readings and was obtained by extrapolation.

TABLE 1. Summary of results from figure 3

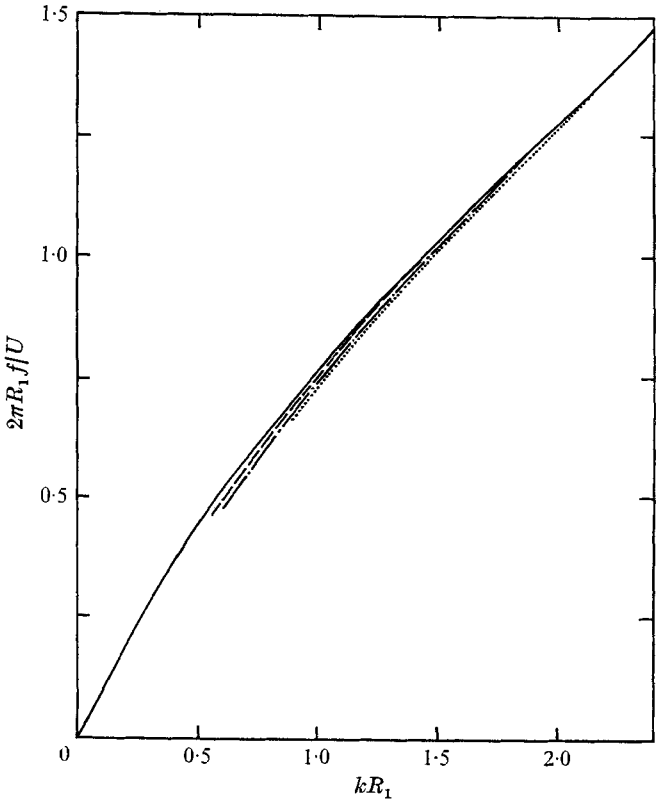

FIGURE 4. Theoretical relationship for instability in a circular slotted tunnel, equation (7): ———, $R_2/R_1 \to \infty$; — — —, $R_2/R_1 = 2{\cdot}87$; —·—·, $R_2/R_1 = 2{\cdot}48$; ·····, $R_2/R_1 = 2{\cdot}33$.

fore adopted. The values of R_1 and R_2 were calculated from (17) and (18) and the values of $f/\bar{V}$ obtained from figure 3 (or table 1); since for the equivalent circular tunnel (7) can be reduced to

$$2\pi f R_1/U = kR_1/(1+\alpha), \tag{19}$$

the value of kR_1, and hence the wavelength λ of the convected disturbance in the shear layer, can be immediately obtained. The variation of $2\pi f R_1/U$ with kR_1 is shown on figure 4, for particular values of R_2/R_1, and a brief summary of the calculations is given in table 2. Once kR_1 is known, the order of magnitude of the neglected complex term in (16) can be estimated from the value of $(\bar{V}-\omega_1/k)^2/gd$, which is also given in table 2. Since $(\bar{V}-\omega_1/k)^2/gd$ never exceeded 0·03, and only rarely exceeded 0·02, the use of (17) to define R_1 appears to be justified.

A comparison of the values of λ calculated in this way with the values expected from (8) and (9) shows immediately that the values of the integer N were 3 and 2 for the lower and higher velocity branches respectively; presumably the velocity was never high enough to activate the basic $N = 1$ mode. A closer numerical comparison shows that the calculated values of λ were always within 8 % of those expected. In fact, the wavelength with the short outer chamber was expected to be fractionally shorter than that forecast from (8), because the short, 1·9 in., length of solid section before the downstream end wall of the outer chamber

	Long outer chamber				Short outer chamber		
Designation on figure 3	(*a*)†	(*b*)†	(*b*)	(*c*)	(*d*)	(*e*)	(*f*)
$2\pi R_1$ (ft) (from equation (17))	3·08	3·85	3·85	4·35	3·08	3·84	4·34
R_2/R_1 (equations (17) and (18))	2·87	2·48	2·48	2·33	2·86	2·48	2·33
$2\pi R_1 f_0/\bar{V}_1$ (from table 1)	0·634	0·737	0·734	0·797	0·576‡	0·660	0·685
$(kR_1)_1$ (corresponding value of kR_1 from figure 4)	0·81	1·00	0·99	1·11	0·72	0·87	0·93
$2\pi R_1 f_0/\bar{V}_2$	0·937	1·098	1·056	1·165	0·861	1·072	1·162
$(kR_1)_2$	1·33	1·65	1·57	1·79	1·20	1·60	1·79
Wavelength λ_1 [$= 2\pi R_1/(kR_1)_1$ (ft)] of shear-layer disturbance for velocity $\bar{V}_1$	3·81	3·87	3·89	3·93	4·29‡	4·42	4·69
Wavelength λ_2 [$= 2\pi R_1/(kR_1)_2$ (ft)] of shear-layer disturbance for velocity $\bar{V}_2$	2·31	2·34	2·46	2·43	2·58	2·40	2·43
Convection velocity $f_0\lambda_1$ [$= \omega_1/k$ (ft/s)] when stream velocity $= \bar{V}_1$	1·49	1·61	1·61	1·71	2·12	2·31	2·54
Convection velocity $f_0\lambda_2$ (ft/s) when stream velocity $= \bar{V}_2$	0·90	0·97	1·02	1·05	1·27	1·26	1·32
$(\bar{V}-\omega_1/k)^2/gd$ when $\bar{V} = \bar{V}_1$	0·012	0·016	0·016	0·016	0·020	0·026	0·030
$(\bar{V}-\omega_1/k)^2/gd$ when $\bar{V} = \bar{V}_2$	0·011	0·012	0·012	0·012	0·018	0·019	0·019
Values of λ (ft) expected from equations (9), long outer chamber, and (8), short outer chamber — $N = 2$	3·85	3·85	3·89	3·89	4·67	4·67	4·67
Values of λ (ft) expected from equations (9), long outer chamber, and (8), short outer chamber — $N = 3$	2·31	2·31	2·34	2·34	2·59	2·59	2·59

† Indicates that velocities were measured with a Pitot tube.

‡ This value occurs slightly above the range of the experimental readings and was obtained by extrapolation.

TABLE 2. Calculations of the wavelength of shear-layer disturbance

probably slightly retards the phase condition imposed on the convected disturbance at the downstream end of the slotted-wall section; this would further improve the agreement. The expected accuracy of (8) and (9) in a resonant feed-back situation is only of order 8 % (Naudascher 1967), and for this reason no attempt was made to allow for the known small experimental errors due to the stationary waves that exist on the flow at Froude numbers above about $\frac{1}{2}$, regardless of the oscillations (Betts & Binnie 1966). Conversely, if (8) and (9) are considered to be accurate, the convection velocities calculated in table 2 are within 8 % or better of the true values, which is again the same order as the agreement between measured and calculated convection velocities obtained by King *et al.*

The above comparison was made in terms of the wavelength of the shear-layer disturbance in order to keep the two distinct elements of the theory separate. When the velocities for natural frequency oscillations are calculated from the expected wavelengths obtained from (8) and (9) the agreement between theory and experiment is slightly better, owing to the shape of the curves on figure 4. The greatest discrepancy, which occurs for the value of $\overline{V}_1$ which had to be extrapolated (figure 3(*d*)), is then only 7 %. If (19) is written as

$$f = \overline{V}/\lambda(1+\alpha) \tag{20}$$

and the wavelength λ of the shear-layer disturbance fixed by the mode number N in (8) or (9), α will be constant for a given depth of water in the flume, and f should vary linearly with $\overline{V}$. The relationships (20) is plotted on figures 3(*a*)–(*f*) for mode numbers 2 and 3. It can be seen that the experimental results of frequency f plotted against stream velocity $\overline{V}$ depart further from these straight lines than do the comparable wind-tunnel results of King *et al.* (their figure 7). This is caused by the resonance being less heavily damped in the flume and consequently requiring a greater phase shift of the forcing mechanism (change in λ) as the frequency of the oscillation is varied from the natural frequency. The stronger resonance in the flume is confirmed by the smaller range of frequencies encountered in these experiments. However, all the comparisons made between theory and experiment are within previously accepted limits, and this justifies the use of the heuristic extension to existing theory and indicates that the basic mechanism of the instability has been correctly understood.

5. Self-induced oscillations in slotted flumes of different scale and form

When the present apparatus is treated as a model for a geometrically similar flume with all linear scales increased by a factor Λ, the scaling is best considered at the natural frequency. Thus, all wavelengths and 'equivalent radii' will also be increased by the factor Λ, and the natural frequency will be reduced in the ratio $1/\Lambda^{\frac{1}{2}}$. Consequently velocities will be scaled as $\Lambda^{\frac{1}{2}}$, and the stream Froude numbers in the model and prototype will be identical. This result can be obtained either from the considerations of §2 or independently by dimensional analysis, if viscous effects are neglected.

A slotted flume is unlikely to be used at stream Froude numbers exceeding

0·55, even if the stationary waves on the flow can be eliminated (Binnie & Cloughley 1970). At the largest depths, which correspond to the probable normal working condition of the flume, both $N = 2$ and $N = 3$ modes occurred at stream Froude numbers less than 0·55 and may be expected to occur at full scale unless they are suppressed. The analysis of §2 makes it possible to consider different configurations of flume. For instance, if the length of the slotted section were increased to 8 ft in the 8ft long outer chamber, the mode of oscillation would be the same as in the short chamber experiments. The wavelength of the shear-layer disturbances would be increased but the natural frequency of oscillation reduced, and the consequent rise in the stream velocity for natural frequency oscillations would only be of order 5 %. Similarly, increasing the depth of the outer chamber, whilst leaving all other dimensions fixed, would increase the natural frequency and hence the corresponding stream velocity by a factor slightly less than $D^{\frac{1}{2}}$. Neither of these modifications is likely to take all oscillations outside the range of Froude numbers less than 0·55.

A full-scale flume is likely to have a nominal open-area ratio of between 9 and 13 %, compared with the $16\frac{2}{3}$ % in the present experiments. Although this will help to weaken the self-induced oscillations (Betts & Binnie 1966), the greater size of the apparatus will have the reverse effect of reducing the dissipation. According to King *et al.* (1958), the reduction in open-area ratio could reduce the ratio of convection to mainstream velocity, and hence slightly increase the velocities at which oscillations occur.

6. Conclusions

The self-induced oscillations observed earlier have been investigated both experimentally and theoretically. Although the theoretical treatment was of necessity heuristic and approximate, the experimental results agreed with the theoretical expectations remarkably well. The theory thus fulfilled the required purpose of making it possible to predict the occurrence of the oscillations in flumes of different geometric form and scale.

The author is grateful to the Hydraulics Research Station, Wallingford, for the use of calibration facilities. He would also like to thank Professor Sir William Hawthorne and the members of the the staff of the University Engineering Department at Cambridge who enabled him to use their facilities for the experiments described in this paper.

REFERENCES

BALDWIN, B. S., TURNER, J. B. & KNECHTEL, E. D. 1954 Wall interference in wind tunnels with slotted and porous boundaries at subsonic speeds. *Nat. Adv. Comm. Aero. Tech. Note*, no. 3176.

BETTS, P. L. & BINNIE, A. M. 1966 Some experiments on ship models held in a small open water-channel with slotted walls. *Trans. Roy. Inst. Nav. Archit.* **108**, 421.

BINNIE, A. M. & CLOUGHLEY, T. M. G. 1970 A comparison of ship-model tests in a slotted-wall channel and in a towing tank. *Trans. Roy. Inst. Nav. Archit.* **112**, 101.

CROW, S. C. & CHAMPAGNE, F. H. 1971 Orderly structure in jet turbulence. *J. Fluid Mech.* **48**, 547.

EAST, L. F. 1966 Aerodynamically induced resonance in rectangular cavities. *J. Sound & Vibration*, **3**, 277.

EDINGTON, J. M. & MOLYNEUX, L. 1960 Portable water velocity meter. *J. Sci. Instrum.* **37**, 455.

FULTZ, D. 1962 An experimental note on finite-amplitude standing gravity waves. *J. Fluid Mech.* **13**, 193.

KING, J. L., BOYLE, P. & OGLE, J. B. 1958 Instability in slotted wall tunnels. *J. Fluid Mech.* **4**, 283.

LIN, C. C. 1955 *The Theory of Hydrodynamic Stability*. Cambridge University Press.

NAUDASCHER, E. 1967 From flow instability to flow-induced excitation. *J. Hydraul. Div. A.S.C.E.* **93**, no. Hy4 (*Proc. Paper*, no. 5336), 15.

RAYLEIGH, LORD 1879 On the instability of jets. *Proc. Lond. Math. Soc.* **10**, 4. (See also *Scientific Papers*, vol. 1, p. 361. Cambridge University Press.)

ROSENHEAD, L. 1931 The formation of vortices from a surface of discontinuity. *Proc. Roy. Soc.* A **134**, 170.

ROSSITER, J. E. 1966 Wind-tunnel experiments on the flow over rectangular cavities at subsonic and transonic speeds. *Aero. Res. Counc. R. & M.* no. 3438.

SATO, H. 1956 Experimental investigation on the transition of laminar separated layer. *J. Phys. Soc. Japan*, **11**, 702.

SATO, H. 1959 Further investigation on the transition of two-dimensional separated layer at subsonic speeds. *J. Phys. Soc. Japan*, **14**, 1797.

TAYLOR, G. I. 1953 An experimental study of standing waves. *Proc. Roy. Soc.* A **218**, 44.

UMIASTOWSKI, J. 1969 The stability of some parallel shear flows. M.Sc. dissertation, University of Manchester.

VANDREY, F. & WIEGHARDT, K. 1955 Experiments on a slotted wall working section in a wind tunnel. *Aero. Res. Counc. Current Paper*, no. 206.

WATSON, G. N. 1944 *A Treatise on the Theory of Bessel Functions*, 2nd edn. Cambridge University Press.